Positioning and time transfer quality in PPP multi-GNSS solutions with constraining of receiver clock parameter

M. Mikoś, K. Sośnica, K. Kazmierski, T. Hadas

Institute of Geodesy and Geoinformatics,
Wrocław University of Environmental and Life Sciences,
Wroclaw, Poland
marcin.mikos@upwr.edu.pl

Wrocław University of Environmental and Life Sciences
IGIG
IGS International GNSS Service

1. Introduction

The International GNSS Service (**IGS**) uses ground stations with various clocks, including internal quartz (**XO**) and external atomic clocks: rubidium (**Rb**), cesium (**Cs**), and hydrogen maser (**HM**). In precise point positioning (**PPP**), estimating receiver clock parameters (**δt_r**) at each epoch adds noise to station coordinates. In **multi-GNSS** solutions (integrating GPS, GLONASS, Galileo, and BeiDou), the receiver clock can be estimated separately for each GNSS or as a **common clock** for one system (e.g. for GPS) with **inter-system biases** (**ISBs**) for other systems. The latter reduces independent clock parameters by a factor of four per epoch. Focusing on IGS stations with HM clocks, we propose using **Markov stochastic process** modeling for receiver clocks via a random walk (**RW**) constraints. Tests on kinematic (**kin** - continuous processing) and static (**sta** - independently for each day) PPP multi-GNSS solutions with varying random walk constraints show that **stochastic clock modeling enhances the stability of station coordinates of HM-equipped GNSS receivers**, positively influencing the final solution outcomes for coordinates and time transfer. **This approach significantly improves the station height component (U), by about 30%**. Fig. 1 indicates the software used; whereas Fig. 2 shows the selected IGS stations.

Fig. 1 Software used in analyses

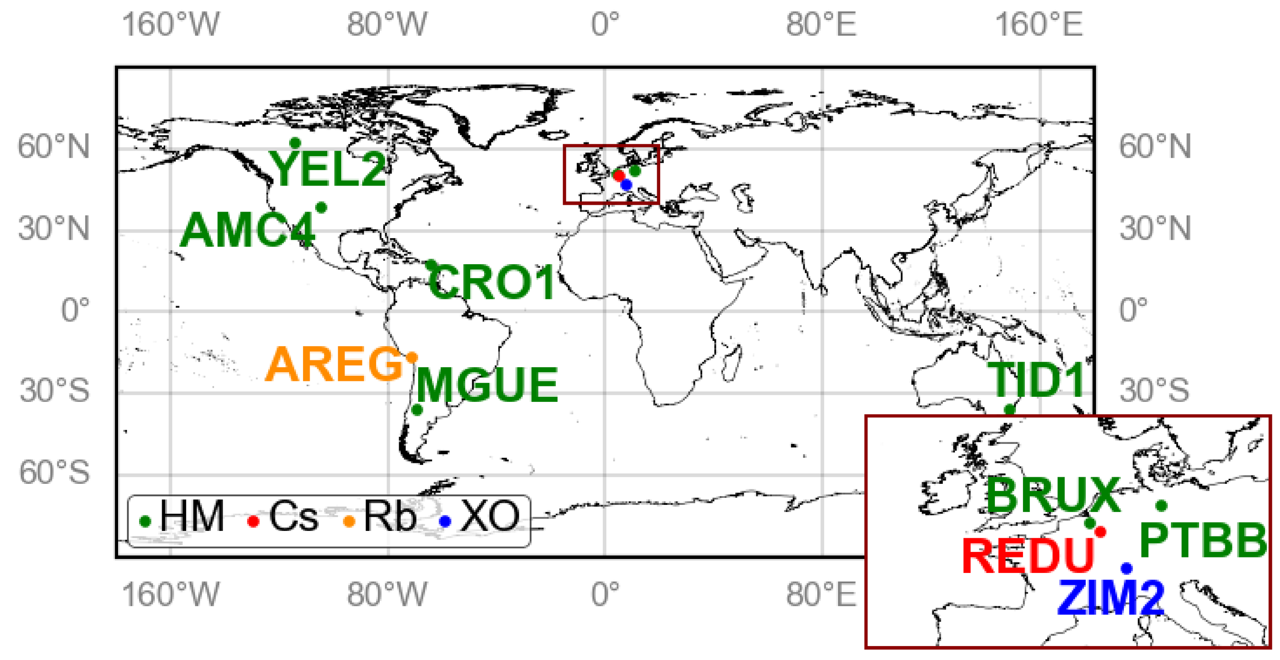

Fig. 2 Multi-GNSS stations equipped with different types of clocks. The color indicates the type of clock. The zoomed part map indicates a part of Europe due to a high concentration of stations

2. Receiver clock parameterization

The process multi-GNSS dual-frequency pseudorange (code) P (Equation 2) and carrier phase L (Equation 1) observations using the undifferenced uncombined model of the PPP technique:

Common Clock (GPS - G) + ISB (GLONASS - R, Galileo - E, BeiDou - C)

$$L_i^s - \rho_0^s + c\delta t^s - \Delta_L^s = \mathbf{e}_r^s \cdot \boldsymbol{\delta X_r} + c\left(\delta t_r^G + ISB_M^G\right) + m^s \cdot T - \frac{f_1^2}{f_i^2} \cdot I^s + \lambda_i \cdot N_i^s \quad (1)$$

$$P_i^s - \rho_0^s + c\delta t^s - \Delta_P^s = \mathbf{e}_r^s \cdot \boldsymbol{\delta X_r} + c\left(\delta t_r^G + ISB_M^G\right) + m^s \cdot T + \frac{f_1^2}{f_i^2} \cdot I^s \quad (2)$$

$$\mathbf{e}_r^s = \left[\frac{X_r - X^s}{\rho_0^s} \quad \frac{Y_r - Y^s}{\rho_0^s} \quad \frac{Z_r - Z^s}{\rho_0^s}\right] \quad (3)$$

$$\boldsymbol{\delta X_r} = \left[\delta X_r \quad \delta Y_r \quad \delta Z_r\right]^T \quad (4)$$

$M \in \{R, E, C\}$

3. Receiver clock modeling

Table 1 Constraints used in RW strategies for the clock parameters and ISB

Strategy	RW [Φ] Common clock (mm)	RW [Φ] ISB (mm)
RV	white noise	static
RW_G	10, 15, 20, 25, 30, 35, 40	static
$RW_{G+ISB}(1)$	10, 15, 20, 25, 30, 35, 40	10, 15, 20, 25, 30, 35, 40
$RW_{G+ISB}(2)$	10, 15, 20, 25, 30, 35, 40	1, 1.5, 2, 2.5, 3, 3.5, 4
$RW_{G+ISB}(3)$	10, 15, 20, 25, 30, 35, 40	0.1, 0.15, 0.2, 0.25, 0.3, 0.35, 0.4

Receiver clock modeling that involves the Markov stochastic process in the form of a RW. Table 1: The unit of the RW process is given in $\frac{m}{\sqrt{s}}$. This means that the constraint of, e.g., 10 mm between neighboring observation epochs corresponds in fact to $\frac{10\ mm}{\sqrt{dt\ s}} = 1.83 \cdot 10^{-3}\ \frac{m}{\sqrt{s}}$, where dt is the time difference between neighboring observation (30 s).

- $\Phi_G : \Phi_{ISB} = 1 : 1$
- $\Phi_G : \Phi_{ISB} = 1 : 0.1$
- $\Phi_G : \Phi_{ISB} = 1 : 0.01$

The most accurate strategies:
RW_G
$RW_{G+ISB}(3)$

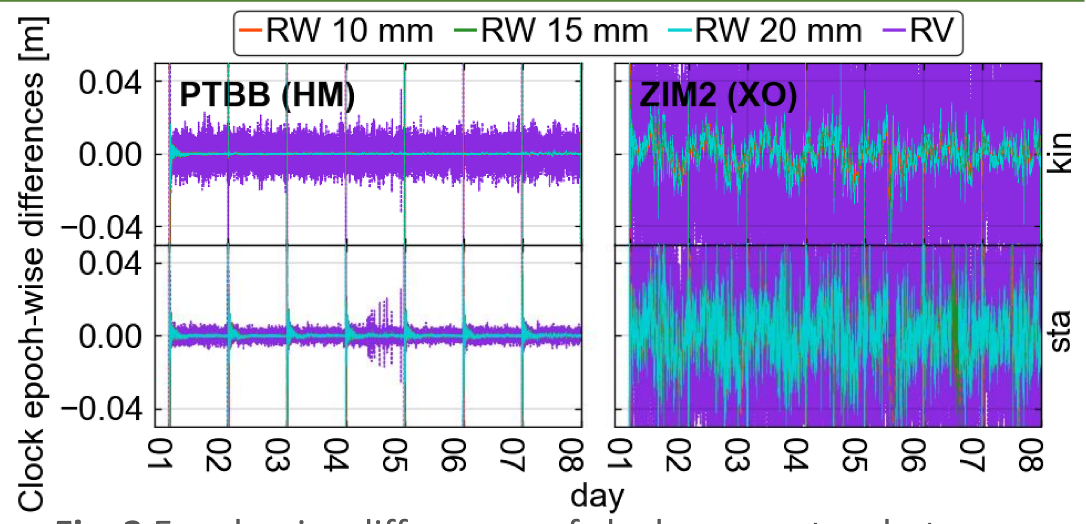

Fig. 3 Epoch-wise differences of clock parameters between adjacent epochs for RW_G and RV (reference) strategies

4. Kinematic PPP solution

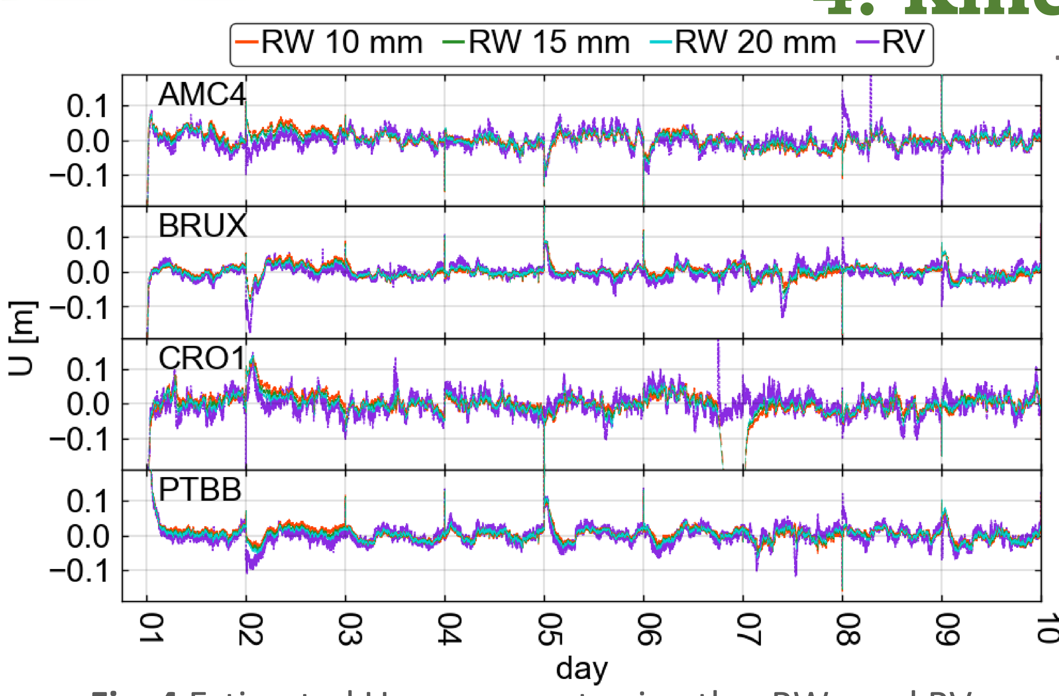

Fig. 4 Estimated U component using the RW_G and RV strategies

Table 2 Median value of the IQR for the coordinates based on kinematic PPP for the entire month from the RW solutions and RV strategy for AMC4, BRUX, CRO1, and PTBB stations

System	Strategy	Coordinate	IQR [mm] Solution – ISB and receiver clock constraint 10 mm	15 mm	20 mm	25 mm	30 mm	35 mm	40 mm	RV Ref.
Multi-GNSS	RW_G	N	11.4	**11.2**	11.2	11.2	11.1	11.1	11.1	**11.2**
		E	14.8	**14.5**	14.4	14.4	14.4	14.4	14.4	**14.4**
		U	24.8	**24.0**	24.5	25.2	25.8	26.3	26.8	**30.3**
	$RW_{G+ISB}(3)$	N	11.4	**11.2**	11.2	11.2	11.1	11.1	11.1	
		E	14.8	**14.5**	14.4	14.4	14.4	14.4	14.4	
		U	24.8	**24.0**	24.6	25.2	25.8	26.2	26.7	

5. Static PPP solution

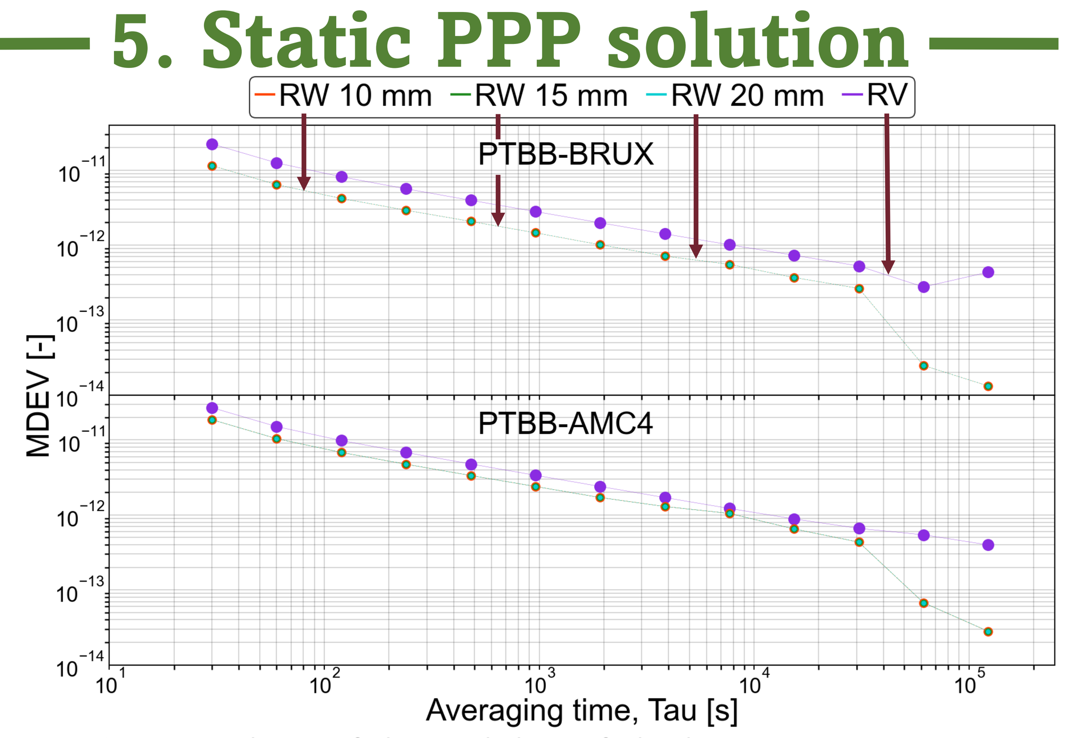

Fig. 5 Analysis of the stability of clock parameters using the RW_G and RV (reference) strategies

6. Test for USN7, USN8, and USN9

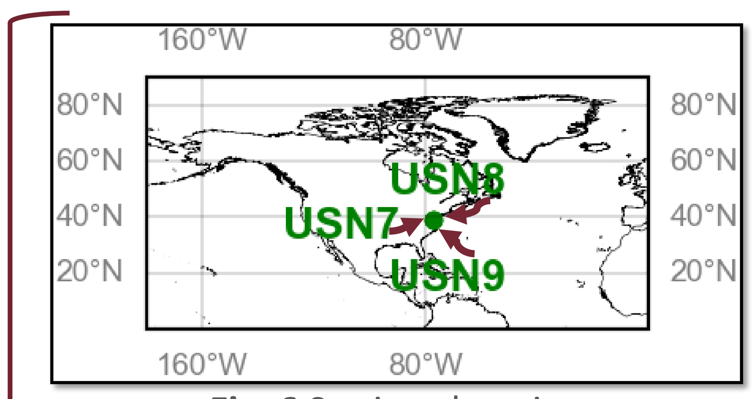

Fig. 6 Stations location

USN7
USN8
USN9

Hydrogen Maser Clock, 10.0 MHz

USN7:
Receiver – SEPT POLARX5TR
Antenna – TPSCR.G5
USN8:
Receiver – SEPT POLARX5TR
Antenna – TPSCR.G5
USN9:
Receiver – NOV OEM6
Antenna – TPSCR.G5

Source: https://network.igs.org/

The purple line overlaps with the blue and green lines.

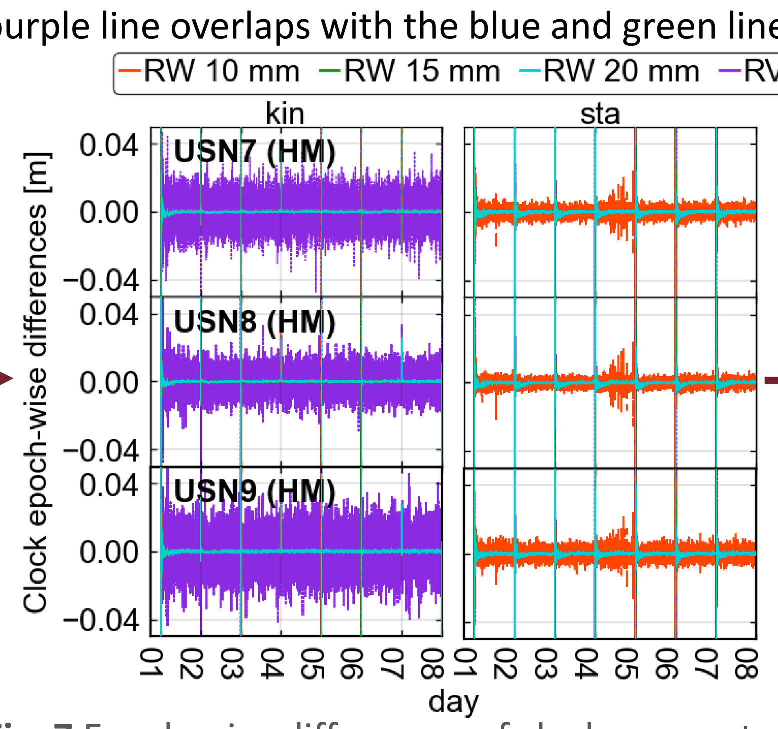

Fig. 7 Epoch-wise differences of clock parameters between adjacent epochs for RW_G and RV strategies

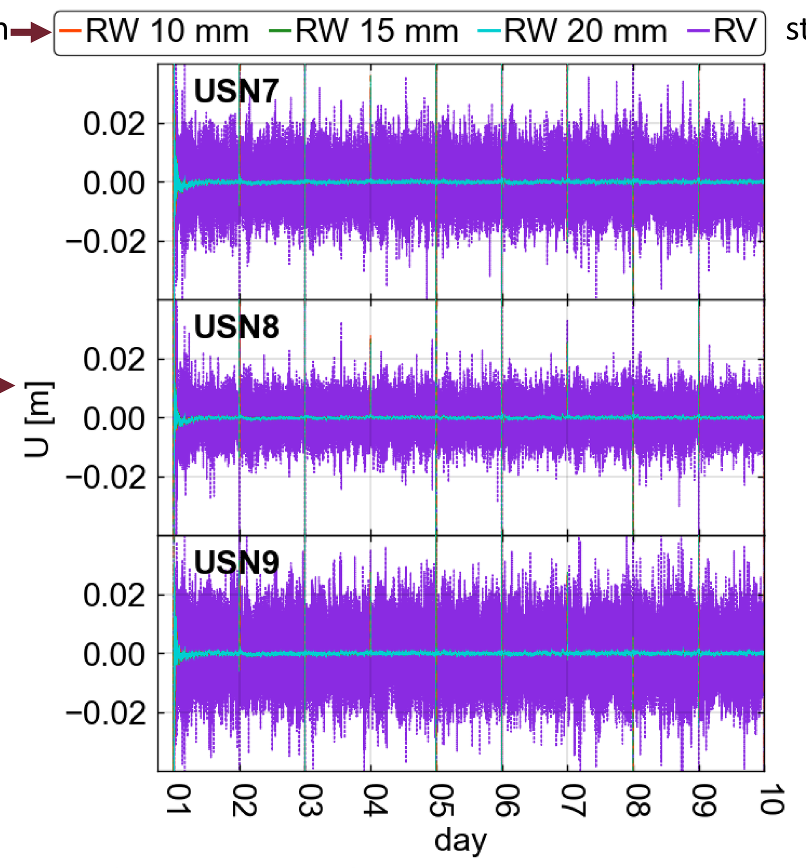

Fig. 8 Estimated U component using the RW_G and RV strategies (**kin**)

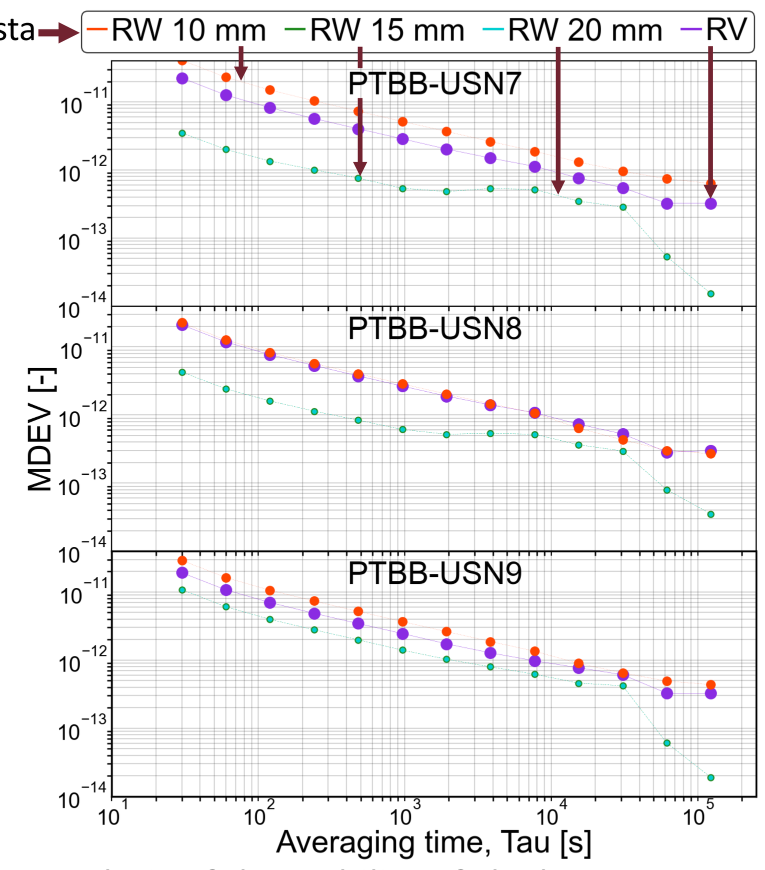

Fig. 9 Analysis of the stability of clock parameters using the RW_G and RV strategies (**sta**)

7. Conclusion

- The most optimal stochastic modeling are **RW_G and $RW_{G+ISB}(3)$** for kinematic multi-GNSS PPP solution (1:0.01 constraint ratio between a common clock and ISB).
- Stochastic modeling is beneficial for the kinematic multi-GNSS PPP solutions for the IGS stations that use hydrogen masers.
- The clock modeling resulted in reduced noise for the estimated clock in the common clock in kinematic multi-GNSS PPP solutions and improved time transfer results.
- **For the kinematic multi-GNSS PPP solution, the most favorable RW constraining is 15 mm.**
- **The improvement in the N and E coordinate components is marginal, but there is a significant improvement in the U component (by up to 30%) in the kinematic multi-GNSS PPP solution.**
- **In the static multi-GNSS PPP solution, the constrained solutions exhibit better both short-term and long-term clock stability in multi-GNSS solutions.**
- The stochastic modeling test has been verified for the co-located GNSS stations equipped with different receiver types: USN7, USN8, and USN9.

8. Acknowledgements

This work was supported by the National Science Centre, Poland (NCN) grant UMO 2018/29/B/ST10/00382, NCN grant UMO 2021/42/E/ST10/00020, and Wrocław University of Environmental and Life Sciences. The IGS and the multi-GNSS Experiment (MGEX) are acknowledged for providing raw GNSS data.

9. Bibliography

1. Mikoś M., Kazmierski K., Sośnica K. (2023) Characteristics of the IGS receiver clock performance from multi-GNSS PPP solutions. GPS Solutions, 27(1), 55, https://doi.org/10.1007/s10291-023-01394-9
2. Mikoś M., Kazmierski K., Hadas T., Sośnica K. (2023) Multi-GNSS PPP solutions with different handling of system-specific receiver clock parameters and inter-system biases. GPS Solutions, 27(3), 137, https://doi.org/10.1007/s10291-023-01474-w
3. Mikoś M., Kazmierski K., Hadas T., Sośnica K. (2024) Stochastic modeling of the receiver clock parameter in Galileo-only and multi-GNSS PPP solutions. GPS Solutions, 28(1), 14, https://doi.org/10.1007/s10291-023-01556-9